Available online at www.sciencedirect.com

ScienceDirect

Ceramics International 40 (2014) 2135–2142

CERAMICS INTERNATIONAL

www.elsevier.com/locate/ceramint

Band gap engineering in $Zn_{(1-x)}Cd_xO$ and $Zn_{(1-x)}Mg_xO$ thin films by RF sputtering

S. Gowrishankar, L. Balakrishnan, N. Gopalakrishnan*

Thin Film Laboratory, Department of Physics, National Institute of Technology, Tiruchirappalli 620015, India

Received 29 March 2013; received in revised form 26 July 2013; accepted 27 July 2013
Available online 2 August 2013

Abstract

Band gap tuning of ZnO by Cd and Mg doping has been investigated. Cd and Mg doped ZnO thin films of different concentrations (0, 3, 10 & 20 mol%) were grown on Si(100) substrates by R.F. magnetron sputtering. The corresponding targets were prepared by the conventional solid-state reaction route. The grown films were characterized by X-ray diffraction (XRD), atomic force microscopy (AFM), Hall effect measurement, photoluminescence (PL), UV–vis–NIR spectroscopy and energy dispersive spectroscopy (EDS). XRD studies showed that all films are preferentially oriented along (002) plane. AFM studies showed that decrease of grain size with the increase of doping concentration. Electrical studies indicate that the resistivity of the films increased by the increase of Cd and Mg concentration. UV–vis–NIR studies showed that the optical band gap of ZnO (3.35 eV) was reduced to 2.74 eV upon Cd alloying while increased to 3.94 eV upon Mg alloying. Red and blue shift in near band edge (NBE) emission observed from PL studies for Cd and Mg alloying respectively, well acknowledged this modulation of band gaps. From modified Vegard's law, the bowing parameter has been estimated to be 1.9 eV and 2.59 eV for Cd and Mg alloyed ZnO films, respectively. The incorporation of dopants (Cd and Mg) in the films has been confirmed by EDS analysis.

Keywords: A. Films; C. Electrical properties; C. Optical properties; D. ZnO

1. Introduction

Large efforts have been promoted on wide-band gap semiconductors because of the intense interest in blue and ultraviolet light emitters & detectors [1]. Among them, ZnO is a universally recognized material for novel optoelectronic, photovoltaic, sensor and nanoelectronic devices [2]. ZnO is a hexagonal wurtzite structure material of direct band gap, 3.36 eV and an excitonic binding energy of 60 meV. The high thermal energy of ZnO (25 meV) leads to the extreme stability of excitons at room temperature and high temperatures [3]. Further, ZnO is a commercially available material having the advantages of low cost, non-toxicity and high chemical stability [4]. Hence, ZnO is considered as a next-generation light-emitting diode (LED) and laser diode (LD) material.

For designing optoelectronic devices, modulation of the band gap is one of major requirements. The band gap of ZnO can be tuned from ultraviolet to visible wavelength by alloying with Cd and Mg, which have been used in solar cells, display panels, sensors, light emitters, ultraviolet light detectors, varistors, etc [5]. ZnO band gap can be engineered by cationic (Cd^{2+} or Mg^{2+}) substitution, which is a versatile tool to tune structural, electrical and optical properties. For narrowing the band gaps, CdO (rock-salt structure) would be an appropriate candidate which has a narrow band gap of 2.38 eV [6]. Alloying with CdO, the band gap of ZnO can be modulated and the luminescence of $Zn_{1-x}Cd_xO$ alloy films can cover the UV to green spectrum. MgO is also a rock-salt structure with a wider band gap of 7.80 eV, which can be alloyed with ZnO for widening the band gaps [7]. By varying the Mg-concentration, the band gap of $Zn_{1-x}Mg_xO$ film can be tuned from 3.36 to 7.80 eV, which cover the wavelength's regions UV-A (320 − 400 nm), UV-B (280 − 320 nm) and UV-C (200 − 280 nm) [8]. In spite of such reports, detailed investigations on Cd and Mg doped ZnO films are necessary.

In this article, we carried out a detailed investigation on structural, optical, electrical and elemental properties of Cd and Mg doped ZnO films of different concentration (0, 3, 10 &

*Corresponding author. Tel.: +91 431 2503607; fax: +91 431 2500133.
E-mail address: ngk@nitt.edu (N. Gopalakrishnan).

0272-8842/$ - see front matter © 2013 Elsevier Ltd and Techna Group S.r.l. All rights reserved.
http://dx.doi.org/10.1016/j.ceramint.2013.07.130

20 mol%) grown by R.F. magnetron sputtering for the band gap tuning study. The light-emitting devices based on ZnCdO/ZnMgO superlattices or quantum wells can confine both excitons and photons in the low dimensions which make the stimulated exciton-related emission process more efficient [9].

2. Experimental

2.1. Preparation of the target

Both CdO and MgO mixed ZnO ceramic targets of different concentrations (3, 10 & 20 mol%) were prepared by conventional solid-state reaction route. For comparison, pure ZnO target was also prepared. Powders of CdO (purity, 99.99%) and MgO (purity, 99.99%) of required stoichiometry were taken with ZnO powder (purity, 99.99%) in a separate bowl with five alumina balls (ball diameter ~15 mm). The bowls were loaded in the ball milling and the powders were blended mechanically for 10 h for the uniform distribution of dopants into ZnO matrix. Then, the mixed powders were calcinated at 900 °C to avoid shrinkage of the target. The calcinated powders of respective target were made into circular disk (target) using hydraulic pellet press at 15 MPa. These discs (pure, Cd & Mg mixed ZnO) were sintered at 950 °C. Thus prepared targets were used as a source material for the film growth. The diameters of the prepared targets are around 55 mm.

2.2. Fabrication of Cd and Mg alloyed ZnO film

Cd doped ZnO (CZO) and Mg doped ZnO (MZO) thin films of different concentrations (0, 3, 10 & 20 mol%) were deposited on the Si (100) substrate by RF magnetron sputtering from CdO and MgO mixed ZnO targets, respectively. The Si (100) substrates of 1×1 cm^2 dimension were cleaned successively by ethanol, acetone, and distilled water in an ultrasonic bath and loaded into the chamber. The distance between substrate and target was kept as 5 cm. The growth chamber was evacuated to a base pressure of 8×10^{-6} mbar. A gas mixture of Ar (sputtering gas) and O_2 (reactive gas) was flown into the chamber by maintaining the total working pressure as 0.02 mbar. The target was pre-sputtered for 10 min to remove the surface contaminations and then, the films were deposited at 450 °C for 30 min at an RF power, 100 W.

The thickness of the grown films was measured by the Filmetrics F20 and is around 100 nm. The structural, electrical, optical and elemental properties of the films were examined by XRD, AFM, Hall effect measurement, UV–vis–NIR spectrometer, PL spectrometer and EDS.

3. Results and discussion

3.1. XRD analysis

The structural properties of the grown films were studied by the XRD (Rigaku Ultima III). Fig. 1 shows the XRD patterns of CZO and MZO films of different concentrations grown on the Si (100) substrate. It is seen that all films are preferentially oriented along (002) plane. Nucleation with various orientations can be formed at an initial stage. Though all nuclei compete to grow, only nuclei having the lowest surface free energy can survive. Thus, the grown films are in (002) preferential orientation as it has the lowest surface free energy [4]. It is worthy to note that no secondary phases have been observed

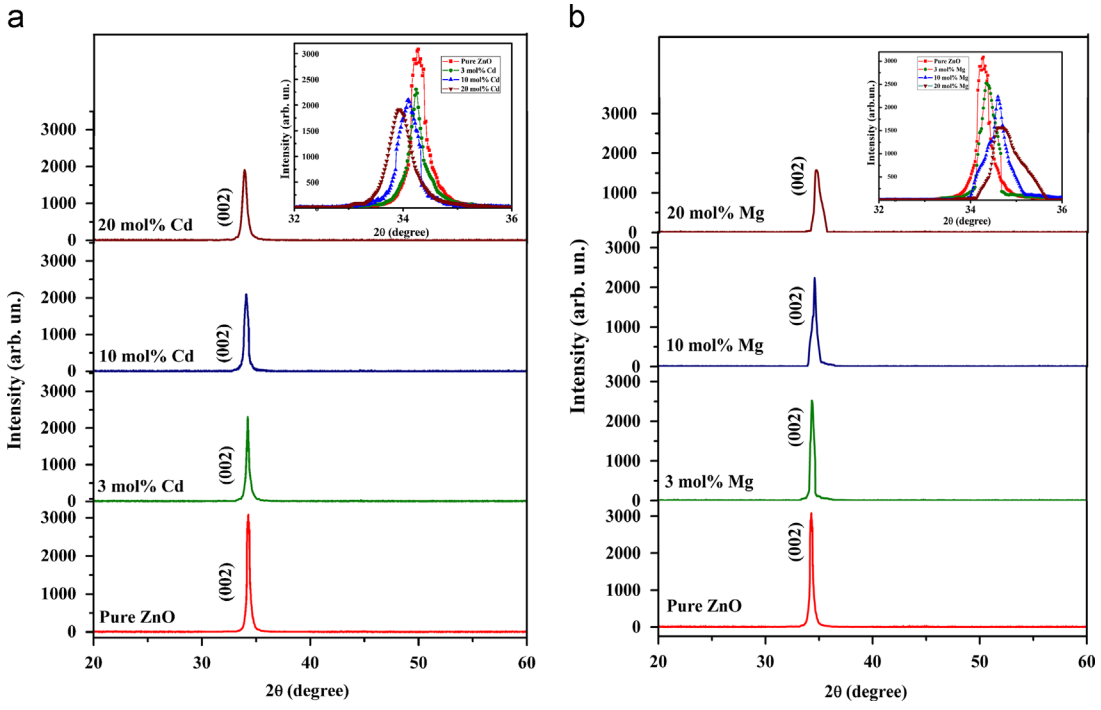

Fig. 1. XRD pattern of (a) Cd doped ZnO thin films (inset: shift in (002) peak) (b) Mg doped ZnO thin films (inset: shift in (002) peak).

Table 1
Lattice constant and crystallite size of Cd and Mg doped ZnO thin films.

Dopants (mol%)	Cd doping			Mg doping		
	Lattice constant 'c' (Å)	Crystallite size (nm)	Thickness (nm)	Lattice constant 'c' (Å)	Crystallite size (nm)	Thickness (nm)
0	5.231	24.7	103	5.231	24.7	103
3	5.238	22.4	100	5.216	21.12	106
10	5.261	19.4	98	5.188	14.37	108
20	5.282	15.4	96	5.159	10.97	110

Table 2
Grain size of Cd and Mg doped ZnO thin films.

Dopants (mol%)	Cd doping Grain size (nm)	Mg doping Grain size (nm)
0	61	61
3	53	49
10	39	33
20	26	24

even at high concentration of MgO or CdO (as both have rocksalt structure). This clearly indicates that both Mg^{2+} and Cd^{2+} ions are dissolved into ZnO. Inset of Fig. 1(a) shows the shift in (002) peak towards a lower angle (34.29° to 33.95°) with the increase of Cd concentration. This is due to the substitution of Zn^{2+} ions (0.60 Å) by high ionic radius Cd^{2+} (0.74 Å) ions [10]. The *c*-axis lattice parameter and crystallite size extracted from XRD have been shown in Table 1. It is seen that the *c*-axis lattice parameter increases monotonically from 5.23 Å to 5.28 Å with the increase of Cd concentration. This unit cell *volume expansion* is due to the ionic radii mismatch between Zn^{2+} and Cd^{2+} ions. Conversely, (002) peak of MZO films shifted towards a higher angle (34.29–34.78°) with the increase of Mg concentration as shown in the inset of Fig. 1(b). The corresponding *c*-axis lattice parameter decreases from 5.23 Å to 5.16 Å as seen in the Table 1. Since the ionic radius of Mg^{2+} (0.57 Å) is smaller than that of Zn^{2+} (0.60 Å), the decrease of the lattice constant implies the substitution of Zn^{2+} by Mg^{2+} ions and hence leads to *volume contraction* of the unit cell [11].

Due to this *volume expansion* and *contraction,* strain has been induced in the films and hence crystalline qualities are deteriorated in both cases. Therefore, the crystallite size decreases both in Cd and Mg doped ZnO films, instead of showing reverse trend (refer Table 1). Otherwise, as there is an ionic radii mismatch in both cases (whether it is a positive or negative mismatch), the crystalline qualities are deteriorated and hence crystallite size decreases.

3.2. Atomic force microscopy

In order to infer about the grain size, atomic force microscope (Agilent 5500) images were recorded. The grain size of pure, Cd and Mg doped ZnO films are shown in the Table 2. From the table, it is noted that the grain size of both Cd and Mg doped films decreases with the increase in doping concentration, which is in similar trend with crystalline size as seen in the XRD analysis. As there is a difference between the atomic size of Cd/Mg and Zn, alloying by Cd or Mg will induce lattice distortion and strain [4]. Hence, Cd/Mg atoms prefer to dwell in and around grain boundary regions to reduce lattice distortion. Thus, the more incorporation of Cd/Mg atoms would prevent grain growth which in turn decreases grain size [12]. Fig. 2 shows the AFM images of pure, 3 mol% Cd and Mg doped ZnO films.

3.3. Electrical analysis

Electrical properties measured by Hall effect measurement (Ecopia HMS 3000) is shown in Table 3. It clearly shows that all the films are *n*-type conductivity with electron concentration almost remains constant. The substitution of isovalent ions Cd^{2+}/Mg^{2+} on Zn^{2+} site does not offer any extra free electrons. Hence, there is not much variation in electron concentration. However, the resistivity gradually increases and mobility decreases with the increase of Cd/Mg concentration. The change in resistivity and mobility has been justified as follows; it is known that ZnO always exhibits *n*-type conductivity. The increase of resistivity with the increase of Cd/Mg concentration might be due to the segregation of Cd/Mg atoms in the grain boundaries which in turn increase the grain boundary barrier [4]. This leads to more scattering of charge carriers at grain boundaries. Thus, the scattering of charge carriers and grain boundary barrier effects causes the increase in resistivity and decrease in mobility upon incorporation of Cd^{2+}/Mg^{2+} ion into ZnO lattice [11]. In addition, the ionic radii mismatch between Cd^{2+} (0.74 Å)/Mg^{2+} (0.57 Å) and Zn^{2+} (0.60 Å) lead to a lattice distortion which in turn increases the resistivity of the films [13,14]. The decrease of grain size (i.e increase of grain boundaries) upon the increase of dopant concentration observed from the AFM analysis also acknowledges our Hall results.

3.4. UV–vis–NIR analysis: (Band gap engineering)

The analysis of optical absorption spectra is one of the most productive tools for understanding the energy band gap (E_g) of crystalline materials. Reflectance spectra were recorded using

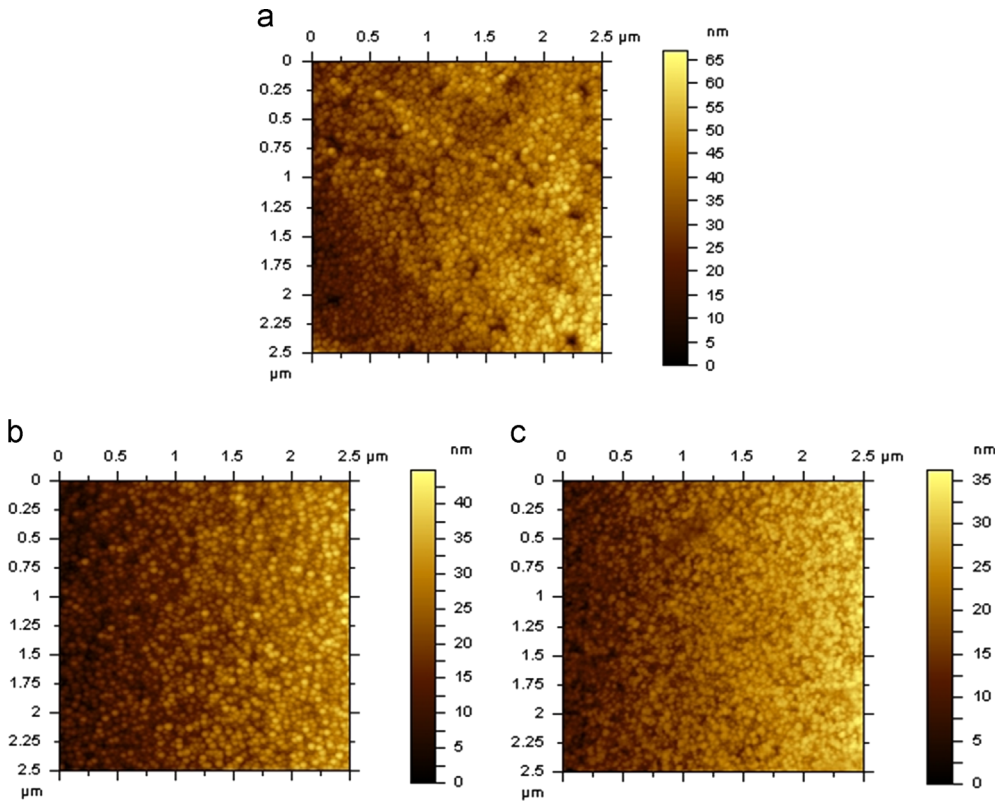

Fig. 2. AFM images of (a) pure ZnO, (b) 3 mol% Cd doped ZnO (3 mol% Zno:Cd) and (c) 3 mol% Mg doped ZnO thin films (3 mol% Zno:Mg).

Table 3
Electrical properties of Cd and Mg doped ZnO thin films.

Dopants (mol%)	Cd doping			Mg doping		
	Electron conc. (cm^{-3})	Resistivity (Ωcm)	Mobility (cm^2/V s)	Electron conc. (cm^{-3})	Resistivity (Ωcm)	Mobility (cm^2/V s)
0	5.37×10^{16}	2	58.19	5.37×10^{16}	2	58.19
3	6.17×10^{16}	5	20.26	5.87×10^{16}	4	26.62
10	4.57×10^{16}	20	6.84	4.77×10^{16}	26	5.04
20	4.15×10^{16}	67	2.25	4.07×10^{16}	55	2.79

UV–vis–NIR spectrometer to obtain the optical band gap from Tauc's plot. The optical energy gap, E_g was calculated by assuming a direct transition between the edges of valence and conduction bands. The variation of the absorption coefficient, α, with photon energy, $h\nu$ is given by the following equation:

$$(\alpha h\nu)^2 = C(h\nu - E_g) \quad (1)$$

where 'α' is the absorption coefficient, 'C' is constant, 'h' is Planck's constant, 'ν' is photon frequency and 'E_g' is the optical band gap [15]. Fig. 3 shows the Tauc's plot of Cd and Mg doped ZnO thin films. By extrapolating the linear region of the $(\alpha h\nu)^2$ versus $(h\nu)$ plot on the x-axis, gives the value of the optical band gap, E_g. It is seen that band gap gradually decreases from 3.35 to 2.74 eV (*red shift*) with the increase of Cd concentration while it increases from 3.35 to 3.94 eV (*blue shift*) with increasing Mg concentration.

Generally, the red and blue shift observed in semiconductors like ZnO, can be explained by Burstein–Moss (BM) effect, i.e. the intentionally doped elements lead to increase or decrease of electrons in the conduction band causes a shift in Fermi level that leads to change in the band gap energy. However, as discussed earlier in the electrical studies, the substitution of Mg^{2+} and Cd^{2+} in the Zn^{2+} sites do not offer any free carriers. Hence, it is presumed that the change (increase/decrease) in the band gap does not associate with the BM effect and related to other factors.

The reason for this red shift/blue shift has been explained as follows; In the case of Cd alloyed ZnO, as the band gap of CdO ($E_g = 2.34$ eV) is lower than ZnO ($E_g = 3.36$ eV), the increase of Cd concentration decreases the band gap. This behavior can be further understood by the fact that the bottom of the conduction band consists of Zn-4s and O-2p states in which Zn-4s states are dominant. With increasing Cd alloying concentrations, the

contribution of Cd-5s states at the bottom of the conduction band becomes stronger which has lower energy than Zn-4s states and hence leads to the lowering of conduction band or band gap narrowing [10,15]. In contrast, in the case of Mg alloyed ZnO, as MgO has higher band gap energy (7.80 eV) than ZnO (3.36 eV), the increase in the Mg incorporation gradually increases the band gap. As Mg^{2+} incorporation increases, the contribution of Mg-3s state becomes dominant at the bottom of the conduction band. Since, the Mg-3s states have higher energy than that of Zn-4s state, the increase of Mg incorporation (Mg-3s states) broadens the optical band gap by heightening the bottom of the conduction band [14].

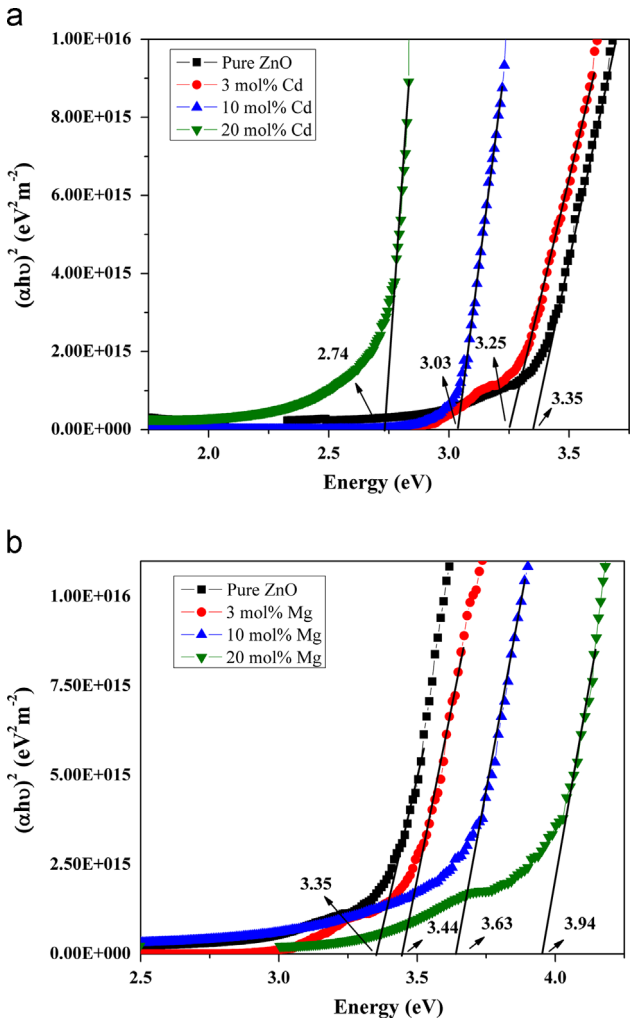

Fig. 3. Tauc's plot of (a) Cd doped ZnO thin films (b) Mg doped ZnO thin films.

The band gap (E_g) of alloyed semiconductors ($A_{1-x}B_xC$) usually deviates from Vegard's linear law [16]. The deviation in the band gap can be described by a modified Vegard's model as,

$$E_{g,\ A_{1-x}B_xC}(x) = xE_{g,\ BC} + (1-x)E_{g,AC} - bx(1-x) \quad (2)$$

where b is optical bowing coefficient and it is vary for different alloyed systems [17]. Following this, the band gap of ternary $Zn_{1-x}Cd_xO$ and $Zn_{1-x}Mg_xO$ alloys can be depicted as a function of the Cd/Mg composition (x) by the following formulae:

$$E_{g,\ Zn_{1-x}Cd_xO}(x) = xE_{g,\ CdO} + (1-x)E_{g,ZnO} - bx(1-x) \quad (3)$$

$$E_{g,\ Zn_{1-x}Mg_xO}(x) = xE_{g,\ MgO} + (1-x)E_{g,ZnO} - bx(1-x) \quad (4)$$

where $E_{g,CdO}$ is the band gap energy of CdO (2.3 eV), $E_{g,MgO}$ is the band gap energy of MgO (7.8 eV) and $E_{g,ZnO}$ is the band gap energy of ZnO (3.36 eV). By substituting our experimental band gap value and corresponding concentration (x) in Eqs. (3) and (4) separately, it is possible to deduce the bowing coefficient 'b' for the CZO and MZO systems. It has been estimated as 2.59 eV for $Zn_{1-x}Cd_xO$ films and 1.9 eV for $Zn_{1-x}Mg_xO$. The bowing parameter is usually deemed to come from three sources, namely, volume deformation, chemical electro negativity difference and internal structural relaxation [18].

Refractive index of the films was calculated using the following equation [19]:

$$[(n^2-1)/(n^2+2)] = 1-(E_g/20)^{1/2} \quad (5)$$

Table 4 shows the variation of band gap and refractive index with respect to dopant concentration. Normally, refractive index depends on the atomic density and atomic masses [20]. It is seen that refractive index of Cd doped films increases with the increase of Cd concentration due to the incorporation of heavier element, Cd (than Zn) in the ZnO matrix. Conversely, the decrease of refractive index with the increase of Mg concentration well agrees with the substitution of lighter element (Mg) in the ZnO matrix.

3.5. Photoluminescence analysis

The optical property of the films was studied by the photoluminescence spectrometer (Perkin Elmer LS 55). Fig. 4 shows the PL spectra of CZO and MZO films. As expected,

Table 4
Band gap and refractive index of Cd and Mg doped ZnO thin films.

Dopants (mol%)	Cd doping		Mg doping	
	Band gap (eV)	Refractive index, *n*	Band gap (eV)	Refractive index, *n*
0	3.35	2.31	3.35	2.31
3	3.25	2.33	3.44	2.28
10	3.03	2.38	3.63	2.24
20	2.74	2.47	3.94	2.18

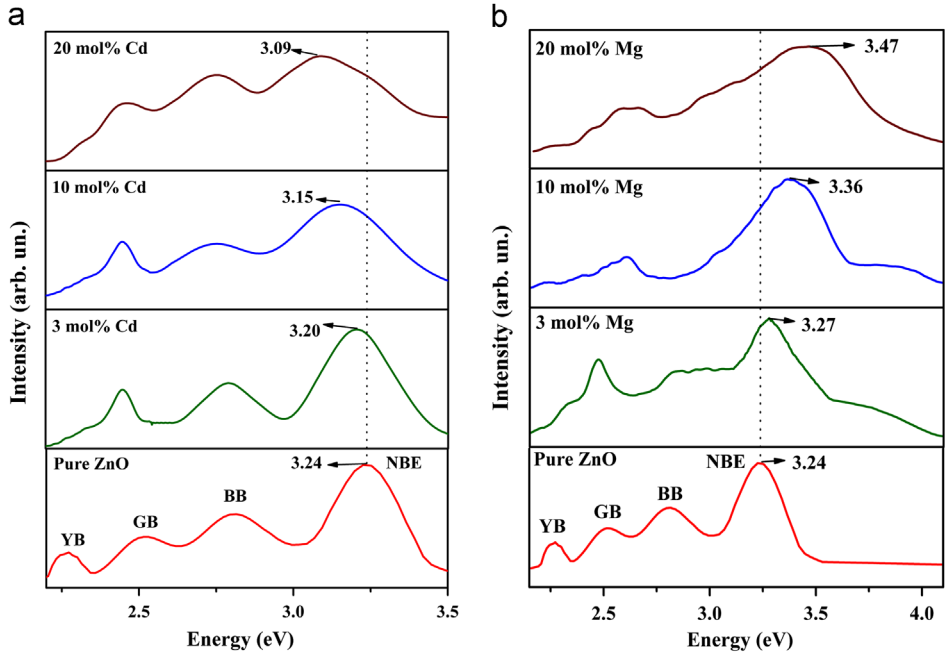

Fig. 4. PL spectra of (a) Cd doped ZnO thin films (b) Mg doped ZnO thin films.

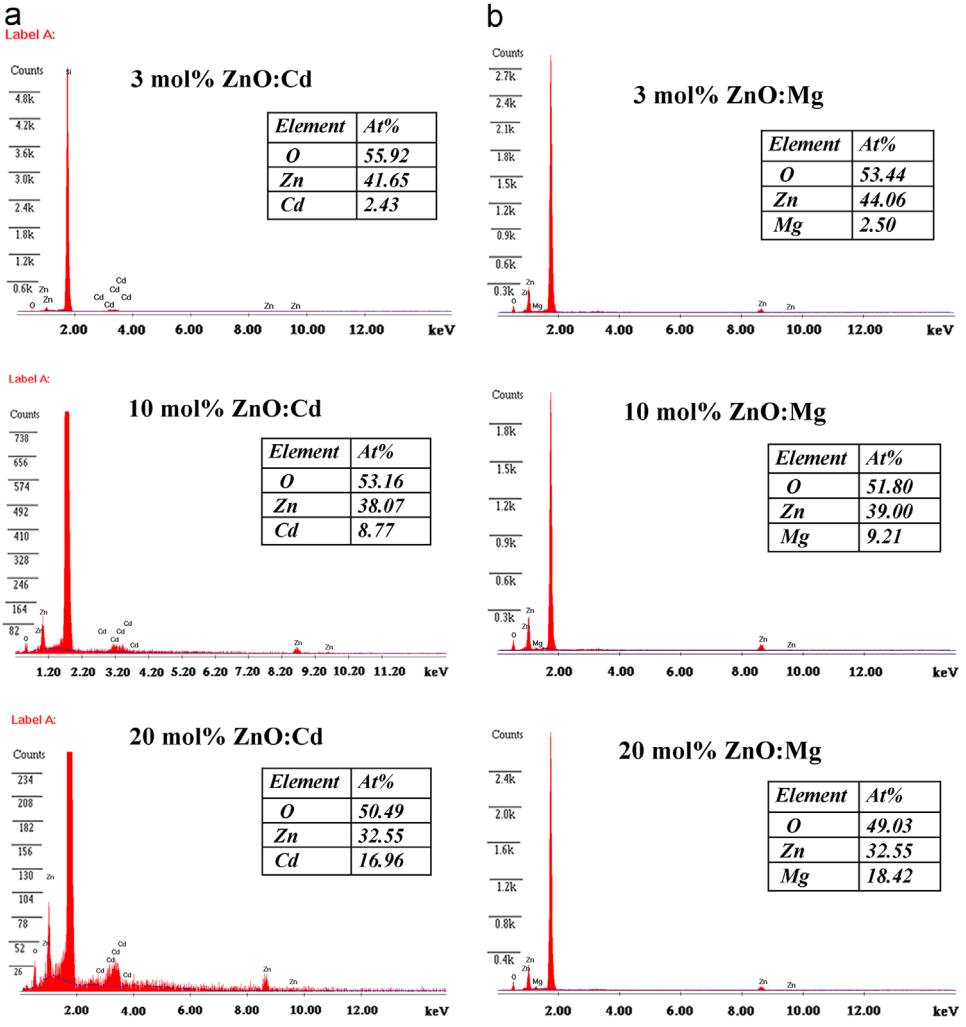

Fig. 5. EDS spectra of (a) Cd doped ZnO thin films (b) Mg doped ZnO thin films.

near-band-edge (NBE) emission has been observed with deep level emissions. These deep levels have been attributed to oxygen vacancies (V_O), interstitial oxygen (O_i), antisite oxygen (O_{Zn}), zinc vacancy (V_{Zn}) and zinc interstitials (Zn_i) [12]. The blue band (BB) is due to the exciton recombination between the electron localized at the zinc interstitials (Zn_i) and the holes in the valence band [13]. Green band (GB) is attributed to singly ionized oxygen vacancies (V_O) and zinc interstitials (Zn_i) [21,22]. The yellow band (YB) is due to oxygen interstitials (O_i) [21].

It is worthy to note that *red shift* in NBE emission was observed for CZO while the *blue shift* for MZO films with the increase of Cd and Mg concentration, respectively. The increase of Cd leads to lowering the conduction band that causes a decrease in the band gap. Thus, the excitation energy for the transition of electrons from the valence band to conduction band becomes small, i.e. the radiative recombination of these excitons may lead to the observed red shift [9]. Similarly, the blue shift due to increase of Mg alloying leads to heightening the bottom of the conduction band that causes the increase of band gap. Hence, the excitation energy for the transition of electrons becomes high and thus leads to blue shift in NBE. The red and blue shifts upon incorporation of Cd and Mg have been also explained in UV–vis–NIR analysis.

The small difference between NBE emission observed from PL and optical band gap observed from Tauc's plot is quite common in alloy semiconductors due to Stokes shift [18,23]. Nevertheless, the observed red and blue shift with the increase of Cd and Mg concentration is well agreed with the modulation of the band gap observed from UV–vis–NIR spectroscopy.

3.6. EDS analysis

In order to confirm the presence of the dopants, CZO and MZO films were subjected to EDS analysis. The EDS spectra shown in Fig. 5(a) and (b) confirms the presence of Cd in CZO and Mg in MZO films, respectively. The compositions of the elements were shown in the insets. It is seen that Cd and Mg concentration in the films have been increases with the increase of their respective doping concentration. It is also noted that concentration of Zn decreases as the doping concentration increases which very well support the substitution of dopants in Zn site. Thus, the EDS result is well acknowledged by our PL and UV–vis–NIR analysis.

4. Conclusion

The band gap engineering in Cd and Mg doped ZnO system has been studied. The films of different concentration were grown on the Si (100) substrate by R.F. magnetron sputtering. The band gap of ZnO (3.35 eV) was tuned to 2.74 eV to 3.94 eV upon Cd and Mg doping. This band gap tuning was well acknowledged by the shift of (002) peak in XRD, NBE shift in PL, decrease of grain size from AFM, variation of resistivity and mobility by Hall measurements and increase of doping concentration in EDS analysis. The tuning of optical band gap of $Zn_{1-x}(Mg,Cd)_xO$ films between 2.74 and 3.94 eV is not only promising for light emitting over a broad spectrum but can be used as a suitable barrier layer/well layer in ZnO based superlattices.

Acknowledgment

This work is supported by Defense Research & Development Organization (DRDO), Govt. of India and is gratefully acknowledged. The authors acknowledged Dr.K.Jeganathan, Center for Nanoscience and Nanotechnology, School of Physics, Bharathidasan univeristy, Tiruchirappalli, India for extending AFM facility.

References

[1] Y.S. Lee, S.N. Lee, I.K. Park, Growth of ZnO hemispheres on silicon by a hydrothermal method, Ceramics International 39 (2013) 3043–3048.
[2] J. Jiang, L. Zhu, Y. Li, Y. Guo, W. Zhou, L. Cao, H. He, Z. Ye, Band gap modulation of ZnCdO alloy thin films with different Cd contents grown by pulsed laser deposition, Journal of Alloys and Compounds 547 (2013) 59–62.
[3] F. Schmidt, H. von Wenckstern, D. Spemann, M. Grundmann, On the radiation hardness of (Mg,Zn)O thin films grown by pulsed-laser deposition, Applied Physics Letters 101 (2012) 012103.
[4] G. Li, X. Zhu, X. Tang, W. Song, Z. Yang, J. Dai, Y. Sun, X. Pan, S. Dai, Doping and annealing effects on ZnO:Cd thin films by sol–gel method, Journal of Alloys and Compounds 509 (2011) 4816–4823.
[5] K. Li, Y. Li, D. Xue, Band gap prediction of alloyed semiconductors, Functional Materials Letters 4 (2011) 217–219.
[6] D.W. Ma, Z.Z. Ye, H.M. Lu, J.Y. Huang, B.H. Zhao, L.P. Zhu, H.J. Zhang, P.M. He, Sputtering deposited ternary $Zn_{1-x}Cd_xO$ crystal films on Si(111) substrates, Thin Solid Films 461 (2004) 250–255.
[7] M. Wei, R.C. Boutwell, J.W. Mares, A. Scheurer, W.V. Schoenfeld, Bandgap engineering of sol–gel synthesized amorphous $Zn_{1-x}Mg_xO$ films, Applied Physics Letters 98 (2011) 261913.
[8] V. Etacheri, R. Roshan, V. Kumar, Mg-doped ZnO nanoparticles for efficient sunlight-driven photocatalysis, Applied Materials and Interfaces 4 (2012) 2717–2725.
[9] Y. Luo, J. Bian, J. Sun, H. Liang, W. Liu, Deposition and tunable photoluminescence of $Zn_{1-x}(Mg,Cd)_xO$ film system, Journal of Materials Processing Technology 189 (2007) 473–476.
[10] B.J. Zheng, J.S. Lian, L. Zhao, Q. Jiang, Structural, optical and electrical properties of $Zn_{1-x}Cd_xO$ thin films prepared by PLD, Applied Surface Science 257 (2011) 5657–5662.
[11] A. Kaushal, D. Kaur, Effect of Mg content on structural, electrical and optical properties of $Zn_{1-x}Mg_xO$ nanocomposite thin films, Solar Energy Materials and Solar Cells 93 (2009) 193–198.
[12] A.D. Acharya, S. Moghe, R. Panda, S.B. Shrivastava, M. Gangrade, T. Shripathi, D.M. Phase, V. Ganesan, Effect of Cd dopant on electrical and optical properties of ZnO thin films prepared by spray pyrolysis route, Thin Solid Films 525 (2012) 49–55.
[13] K. Huang, Z. Tang, L. Zhang, J. Yu, J. Lv, X. Liu, F. Liu, Preparation and characterization of Mg-doped ZnO thin films by sol–gel method, Applied Surface Science 258 (2012) 3710–3713.
[14] S. Snega, K. Ravichandran, N. Jabena Begum, K. Thirumurugan, Enhancement in the electrical and antibacterial properties of sprayed ZnO films by simultaneous doping of Mg and F, Journal of Materials Science—Materials in Electronics 24 (2013) 135–141.
[15] X.D. Zhang, M.L. Guo, W.X. Li, C.L. Liu, First-principles study of electronic and optical properties in wurtzite $Zn_{1-x}Cd_xO$, Journal of Applied Physics 103 (2008) 063721.
[16] A. Schleife, C. Rödl, J. Furthmüller, F. Bechstedt, Electronic and optical properties of $Mg_xZn_{1-x}O$ and $Cd_xZn_{1-x}O$ from *ab initio* calculations, New Journal of Phys 13 (2011) 085012.

[17] X.F. Fan, H.D. Sun, Z.X. Shen, J.L. Kuo, Y.M. Lu, A first-principle analysis on the phase stabilities, chemical bonds and band gaps of wurtzite structure $A_xZn_{1-x}O$ alloys (A=Ca, Cd, Mg), Journal of Physics Condensed Matter 20 (2008) 235221.

[18] D.W. Ma, Z.Z. Ye, Y.S. Yang, Photoluminescent analysis of $Zn_{1-x}Cd_xO$ alloys, Applied Physics B 82 (2006) 85–87.

[19] H. Benzarouk, A. Drici, M. Mekhnache, A. Amara, M. Guerioune, J.C. Bernède, H. Bendjffal, Effect of different dopant elements (Al, Mg and Ni) on microstructural, optical and electrochemical properties of ZnO thin films deposited by spray pyrolysis (SP), Superlattices and Microstructures 52 (2012) 594–604.

[20] G. Epurescu, R. Birjega, A.C. Galca, Tailoring the optical properties of $Mg_xZn_{1-x}O$ thinfilms by nitrogen doping, Applied Physics A 104 (2011) 889–893.

[21] J.H. Hong, Y.F. Wang, G. He, J.X. Wang, Tuning visible emission by choosing excitation wavelength in Mg-doped ZnO/silica composites, Journal of Alloys and Compounds 506 (2010) 1–3.

[22] S.K. Lee, J.Y. Son, Epitaxial growth of thin films and nanodots of ZnO on Si (111) by pulsed laser deposition, Applied Physics Letters 100 (2012) 132109.

[23] T.H. Kim, J.J. Park, S.H. Nam, H.S. Park, N.R. Cheong, J.K. Song, S.M. Park, Fabrication of Mg-doped ZnO thin films by laser ablation of Zn:Mg target, Applied Surface Science 255 (2009) 5264–5266.